Electronic Supplementary Material (ESI) for Green Chemistry.
This journal is © The Royal Society of Chemistry 2021

Supplementary Information

Solvent Effect on Xylose-to-Furfural Reaction in Biphasic Systems: Combined Experiments with Theoretical Calculations

Qixuan Lin,[a] Qiwen Zhan[a], Rui Li[a], Shouwei Liao,[b] Junli Ren,[a,*] Feng Peng,[c] Libo Li[b,*]

[a]State Key Laboratory of Pulp and Paper Engineering, South China University of Technology, Wushan Road, Tianhe District, Guangzhou 510640, China.

[b]School of Chemistry and Chemical Engineering, South China University of Technology, Wushan Road, Tianhe District, Guangzhou 510640, China

[c]Beijing Key Laboratory of Lignocellulosic Chemistry, Beijing Forestry University, East Qinghua Road, Haidian District, Beijing, 100083, China

***Email:** renjunli@scut.edu.cn; celbli@scut.edu.cn;

Molecular Dynamics Simulation

Molecular dynamics (MD) simulation was performed using GROMACS 5.1.4 package.[1-3] OPLS topology data for molecules were obtained from LigParGen, a free web service offered by Jorgensen research group.[4-6] In the simulations, xylose and furfural molecules (solute), were solvated in six biphasic systems, respectively (the water and organic solvent volume ratio is 1:1). The simulation box sizes were ~3.0 nm with PBC (periodic boundary condition) applied to all 3 dimensions of the system. The OPLS/AA force-field[6, 7] was employed to model the xylose, furfural and organic solvent molecules, while TIP4P[8] model was used to describe the water molecule. Each system was simulated for 25 ns in an NVT ensemble with an integration time step of 2 fs and the last 20 ns was used for the subsequent analysis. This was preceded by a 5 ns of NPT equilibration MD run. Steepest-descent energy minimization was performed before the NPT MD simulation to remove accidental overlaps. All the simulation systems were maintained at 298 K using the v-rescale thermostat.[9] A time constant of 0.1 ps was applied for the temperature coupling. The Lennard-Jones (LJ) interactions were switched off smoothly between 10 and 12 Å, and a long-range analytical dispersion correction[10] was applied to the energy and pressure to account for the truncation of LJ interactions. The neighbour list was updated every 0.01 ps within 1.2 nm. The electrostatic interactions were evaluated with a real-space cutoff of 12 Å, with the long-range component calculated with the PME (Particle Mesh Ewald) method.[11] LINCS[12] algorithm was used to constraint the bonds involving hydrogen atoms, and SETTLE[13] algorithm was employed to constraint water geometry. The simulation trajectory data (saved every 2ps) were analyzed with the GROMACS package, with figures produced by the VMD[14] software. The Z-axis coordinates of xylose and furfural over time, radial distribution functions (RDF), spatial density functions (SDF), and hydrogen bonds (H-bonds) between solute and solvents were calculated. As for other simulation details, please refer to our previous publications.[15, 16]

Table S1. The partition coefficient of furfural in the biphasic systems during reaction

Systems	Time (min)	Partition coefficient		
		170°C	180°C	190°C
2-Butanol/H_2O	40	362	65	6
	60	66	9	5
	80	12	8	30
	100	12	7	4
2-MTHF/H_2O	40	242	68	10
	60	114	4	9
	80	15	22	9
	100	18	14	8
CPME/H_2O	40	208	33	3
	60	20	5	2
	80	5	5	4
	100	6	4	3
Toluene/H_2O	40	21	10	2
	60	9	3	2
	80	6	5	3
	100	4	4	3
MIBK/H_2O	40	195	42	25
	60	62	23	10
	80	22	20	15
	100	16	15	15
DCM/H_2O	40	22	16	6
	60	8	32	15
	80	12	19	19
	100	12	16	266

Table S2. Kinetics parameters for xylose conversion in the six biphasic systems

Solvent system	Temp.	$k_1(min^{-1})$	$k_2(min^{-1})$	$k_3(min^{-1})$	$k_4(min^{-1})$
	170°C	0.011	27.28	1.65×10^{-11}	0.025
2-Butanol/H_2O	180°C	0.0086	92.17	0.015	0.0058
	190°C	0.0066	92.12	0.020	3.19×10^{-9}
	170°C	0.016	22.34	1.32×10^{-13}	0.018
2-MTHF/H_2O	180°C	0.0089	44.76	0.013	8.46×10^{-16}
	190°C	0.0064	35.34	0.016	1.88×10^{-16}
	170°C	0.0050	29.80	0.0022	0.013
CPME/H_2O	180°C	0.0082	60.08	0.0032	0.025
	190°C	0.0037	40.89	0.0091	2.03×10^{-16}
	170°C	0.0041	92.12	0.0091	4.29×10^{-18}
Toluene/H_2O	180°C	0.0073	92.13	0.0034	0.040
	190°C	0.0032	92.10	0.0137	4.42×10^{-17}
	170°C	0.011	37.85	4.18×10^{-12}	0.026
MIBK/H_2O	180°C	0.0075	91.44	0.013	2.77×10^{-14}
	190°C	0.0099	92.13	0.014	1.13×10^{-16}
	170°C	0.021	91.44	0.0154	1.56×10^{-13}
DCM/H_2O	180°C	0.077	92.47	2.21×10^{-12}	0.017
	190°C	0.050	92.98	0.058	0.013

Table S3. The solvation free energy (ΔG_{sol}) of furfural in various solvents

Solvents	**ΔG_{sol} in the first 1 ns (kJ/mol)**	**ΔG_{sol} in the first 2 ns (kJ/mol)**	**ΔG_{sol} in the first 3 ns (kJ/mol)**	**ΔG_{sol} in the first 4 ns (kJ/mol)**
Water	-17.32±0.40	-17.22±0.26	-16.84±0.26	-16.89±0.26
Toluene	-23.42±0.27	-23.55±0.22	-23.56±0.12	-23.53±0.15
MIBK	-26.17±0.31	-26.29±0.15	-26.43±0.20	-26.34±0.13
CPME	-30.71±0.26	-30.53±0.15	-30.46±0.25	-30.54±0.15
2-MTHF	-30.48±0.20	-30.39±0.27	-30.73±0.19	-30.62±0.12
2-Butanol	-33.93±0.43	-34.56±0.59	-34.39±0.36	-34.09±0.44
DCM	-37.93±0.22	-37.62±0.24	-37.44±0.17	-37.39±0.18

Table S4. The solvation free energy of furfural in various solvents

Systems	Total ΔG_{sol} (kJ/mol)[b]	Polar ΔG_{sol} (kJ/mol)[b]	Nonpolar ΔG_{sol} (kJ/mol)[b]
FF[a] in water	-16.89±0.26	-24.14±0.07	7.25±0.20
FF[a] in toluene	-23.53±0.15	-11.38±0.08	-12.15±0.18
FF[a] in MIBK	-26.34±0.13	-13.19±0.08	-13.16±0.14
FF[a] in CPME	-30.54±0.15	-11.64±0.07	-18.90±0.12
FF[a] in 2-MTHF	-30.62±0.12	-10.13±0.04	-20.49±0.10
FF[a] in 2-butanol	-34.09±0.44	-15.57±0.20	-18.52±0.26
FF[a] in DCM	-37.39±0.18	-18.74±0.14	-18.65±0.06

[a]FF: Furfural. [b]ΔG_{sol}: Solvation free energy.

Table S5. λ Schedule*

Window index	1	2	3	4	5	6	7	8	9	10	11	12	13	14
λ_{vdw}	0	0	0	0	0.1	0.2	0.3	0.4	0.5	0.6	0.7	0.8	0.9	1
λ_{coul}	0	0.25	0.50	0.75	1	1	1	1	1.	1	1	1	1	1

*The λ_{vdw} and λ_{coul} refer to the scaling the van der Waals and Coulombic interactions, respectively, at each window.

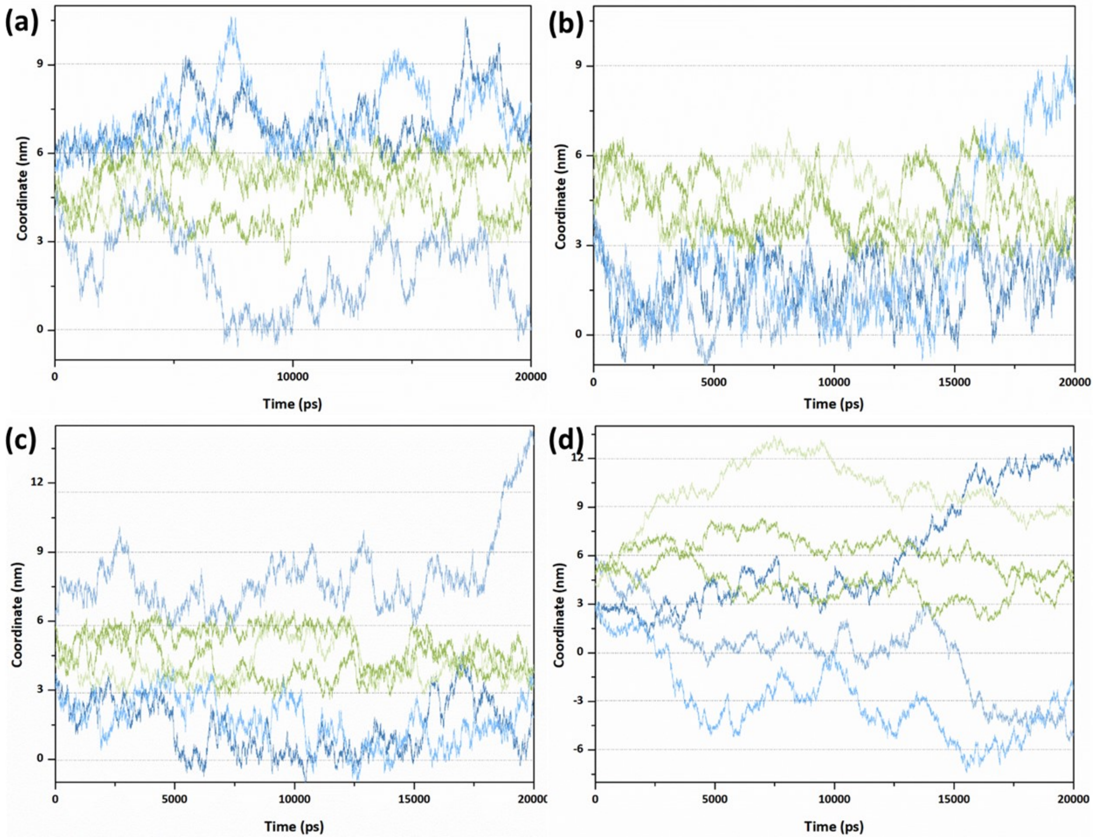

Figure S1. The moving trajectories of furfural and xylose in Z-axis in (a) MIBK/H_2O, (b) 2-MTHF/H_2O, (c) CPME/H_2O, and (d) 2-butanol/H_2O systems. Dotted lines show the boundary between the aqueous and organic phases. Initially, the organic phase is in the range of 0-3 nm, and the aqueous phase is in the range of 3-6 nm on the Z axis. The two phases cycle alternately. Blue: furfural; Green: xylose.

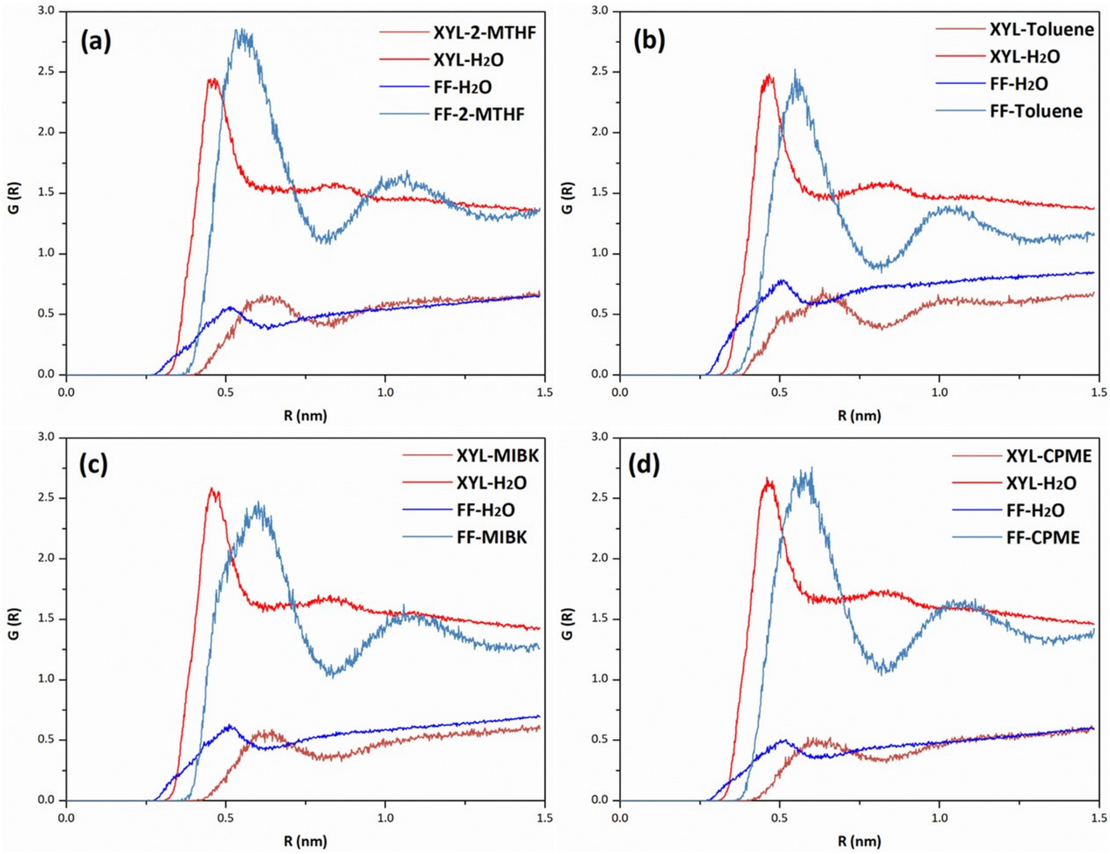

Figure S2. Centre of mass radial distribution functions (RDF) of solvent molecules with respect to xylose or furfural

References

1. B. Hess, C. Kutzner, D. van der Spoel and E. Lindahl, *Journal of Chemical Theory and Computation*, 2008, **4**, 435-447.
2. H. J. C. Berendsen, D. van der Spoel and R. van Drunen, *Computer Physics Communications*, 1995, **91**, 43-56.
3. D. Van Der Spoel, E. Lindahl, B. Hess, G. Groenhof, A. E. Mark and H. J. C. Berendsen, *Journal of Computational Chemistry*, 2005, **26**, 1701-1718.
4. W. L. Jorgensen and J. Tirado-Rives, *Proceedings of the National Academy of Sciences of the United States of America*, 2005, **102**, 6665-6670.
5. L. S. Dodda, J. Z. Vilseck, J. Tirado-Rives and W. L. Jorgensen, *The Journal of Physical Chemistry B*, 2017, **121**, 3864-3870.
6. L. S. Dodda, I. Cabeza de Vaca, J. Tirado-Rives and W. L. Jorgensen, *Nucleic acids research*, 2017, **45**, W331-W336.
7. M. J. Robertson, J. Tirado-Rives and W. L. Jorgensen, *Journal of Chemical Theory and Computation*, 2015, **11**, 3499-3509.
8. W. L. Jorgensen and J. D. Madura, *Molecular Physics*, 1985, **56**, 1381-1392.
9. G. Bussi, D. Donadio and M. Parrinello, *The Journal of Chemical Physics*, 2007, **126**, 014101.
10. M. R. Shirts, J. W. Pitera, W. C. Swope and V. S. Pande, *The Journal of Chemical Physics*, 2003, **119**, 5740-5761.
11. T. Darden, D. York and L. Pedersen, *The Journal of Chemical Physics*, 1993, **98**, 10089-10092.

12. B. Hess, H. Bekker, H. J. C. Berendsen and J. G. E. M. Fraaije, *Journal of Computational Chemistry*, 1997, **18**, 1463-1472.
13. S. Miyamoto and P. A. Kollman, *Journal of Computational Chemistry*, 1992, **13**, 952-962.
14. W. Humphrey, A. Dalke and K. Schulten, *Journal of Molecular Graphics*, 1996, **14**, 33-38.
15. H. Chen, L. Li, T. Zhang, Z. Qiao, J. Tang and J. Zhou, *The Journal of Physical Chemistry C*, 2018, **122**, 2070-2080.
16. L. Li, C. J. Fennell and K. A. Dill, *The Journal of Physical Chemistry B*, 2014, **118**, 6431-6437.